

Normal state resistivity of $\text{Ba}_{1-x}\text{K}_x\text{Fe}_2\text{As}_2$: evidence for multiband strong-coupling behavior

A. A. Golubov[◦], O. V. Dolgov[△], A. V. Boris[△], A. Charnukha[△], D. L. Sun[△], C. T. Lin[△], A. F. Shevchun[□],
A. V. Korobenko^{□▽}, M. R. Trunin^{□▽}, V. N. Zverev^{□▽}

[◦]Faculty of Science and Technology and MESA+ Institute for Nanotechnology, University of Twente, Enschede, The Netherlands

[△]Max-Planck-Institut für Festkörperforschung, D-70569 Stuttgart, Germany

[□]Institute of Solid State Physics, Chernogolovka, Russia

[▽]Moscow Institute of Physics and Technology, Dolgoprudny, Russia

Submitted 25 April 2011

Resubmitted 7 July 2011

We present theoretical analysis of the normal state resistivity in multiband superconductors in the framework of Eliashberg theory. The results are compared with measurements of the temperature dependence of normal state resistivity of high-purity $\text{Ba}_{0.68}\text{K}_{0.32}\text{Fe}_2\text{As}_2$ single crystals with the highest reported transition temperature $T_c = 38.5$ K. The experimental data demonstrate strong deviations from the Bloch–Grüneisen behavior, namely the tendency to saturation of the resistivity at high temperatures. The observed behavior of the resistivity is explained within the two band scenario when the first band is strongly coupled and relatively clean, while the second band is weakly coupled and is characterized by much stronger impurity scattering.

Introduction. It is widely known that many disordered alloys exhibit resistivity saturation [1, 2]. In order to describe these data, phenomenological model was suggested which assumed the existence of an effective shunt with large temperature-independent resistance. This model assumes the existence of two parallel conductivity channels, i.e. two groups of carriers having different scattering parameters:

$$\rho^{-1} = \rho_0^{-1} + \rho_{sh}^{-1}, \quad (1)$$

where ρ_0 is the resistivity of the first group of carriers which is characterized by weak scattering on static defects and by large slope of temperature dependence of resistivity (strong temperature-dependent scattering) and ρ_{sh} is the resistivity of the second group (shunt) characterized by strong temperature-independent scattering of carriers. This simple approach provides good fit to experimental data [1–3] but it was never justified on physical grounds (see the discussion in review [4]). Resistivity saturation was also observed in previous studies of V_3Si compounds [5, 6] and an empirical explanation was suggested in [5] to explain this effect, however no physical basis for such approach was provided.

The newly discovered iron pnictide superconductors [7] present an unusual case of multiband superconductivity. Currently, there is accumulating evidence in favor of multiband effects and pairing mechanism due to exchange of magnetic fluctuations connecting different sets of Fermi surfaces [8–11]. Apart of superconducting be-

havior, normal state properties of pnictides also attract a lot of interest. Recent measurements of normal state resistivity and Hall effect revealed a number of anomalous features. While the resistivity of Co-doped BaFe_2As_2 compounds follows standard Bloch–Grüneisen law above T_c [12, 13], in K- and Ru-doped BaFe_2As_2 , as well as in LiFeAs and SrPt_2As_2 compounds the resistivity exhibit a tendency to saturation [14–18]. In addition, Hall coefficient in these materials is temperature-dependent.

In the present work we will argue that the effective shunt model can be derived for hole-doped pnictides and it explains the resistivity saturation observed in these compounds. The model is based on our knowledge of electronic structure of pnictides. In Ref. [19], a microscopic calculation of the specific heat in the framework of a four band Eliashberg spin-fluctuation model was performed. These four bands correspond to two electron pockets and two hole pockets. It was further shown in [19] that two effective bands can be constructed by combining two electronic pockets and inner hole pocket (around Γ -point) into one band, while the remaining outer hole pocket forms the second band. Important result is that the second band is characterized by much weaker interaction of carriers with intermediate bosons (presumably spin fluctuations) than the first one, since nesting conditions are not fulfilled for the outer hole pocket. Further, the authors of Ref. [13] reached important conclusion that relaxation rates of the holes in $\text{Ba}(\text{Fe}_{1-x}\text{Co}_x)_2\text{As}_2$ are much higher than relaxation

rates of the electrons, as follows from their analysis of Hall effect in this compound. As a result, the outer hole pocket is characterized by weak interaction between carriers and strong temperature-independent scattering and thus provides the physical realization of effective shunting resistor in the model [1–4].

In this work we perform theoretical analysis of a normal state resistivity and compare it with the data for *dc* and microwave resistivity measurements in $\text{Ba}_{0.68}\text{K}_{0.32}\text{Fe}_2\text{As}_2$ single crystals with highest available critical temperature $T_c = 38.5$ K. The proposed multi-band scenario is also consistent with our Hall-effect measurements on the same $\text{Ba}_{0.68}\text{K}_{0.32}\text{Fe}_2\text{As}_2$ single crystals. Our model also provides explanation of the difference between resistivities in K- and Co-doped BaFe_2As_2 in terms of stronger impurity scattering within electronic pockets in Co-doped compounds.

Single band case. The *DC*-resistivity in the single band model is determined by the expression [20, 21]

$$\rho_{DC}(T) = \left[\frac{\epsilon_0 \omega_{pl}^2}{W} \right]^{-1}, \quad (2)$$

where ω_{pl} is a bare (band) plasma frequency, and the kernel $W(T)$ is determined by the impurity scattering rate γ^{imp} and the Bloch–Grüneisen integral of the *transport* Eliashberg function $\alpha_{tr}^2(\Omega)F(\Omega)$

$$W = \gamma^{\text{imp}} + \frac{\pi}{\beta T} \int_0^\infty d\Omega \frac{\Omega}{\sinh^2(\Omega/2\beta T)} \alpha_{tr}^2(\Omega) F(\Omega), \quad (3)$$

where $\beta = k_B/\hbar$. To simplify notations, below we will skip the subscript “*tr*” in the transport Eliashberg function and coupling constants.

Two band case. In the two-band case the above expression for the resistivity can be straightforwardly extended by adding the conductivities of both bands

$$\rho_{DC}(T) = \left[\frac{\epsilon_0 \omega_{pl1}^2}{W_1} + \frac{\epsilon_0 \omega_{pl2}^2}{W_2} \right]^{-1}, \quad (4)$$

$$W_i = \gamma_i^{\text{imp}} + \frac{\pi}{\beta T} \int_0^\infty d\Omega \frac{\Omega}{\sinh^2(\Omega/2\beta T)} \alpha_i^2(\Omega) F_i(\Omega), \quad (5)$$

where $i = 1, 2$. In the above expression the scattering parameters are defined as $\gamma_1^{\text{imp}} = \gamma_{11}^{\text{imp}} + \gamma_{12}^{\text{imp}}$ and $\gamma_2^{\text{imp}} = \gamma_{21}^{\text{imp}} + \gamma_{22}^{\text{imp}}$, where $\gamma_{11}^{\text{imp}}, \gamma_{12}^{\text{imp}}$ and $\gamma_{21}^{\text{imp}}, \gamma_{22}^{\text{imp}}$ are, respectively, *intra*band and *inter*band scattering rates.

At high temperatures, $T \gtrsim \tilde{\Omega}/5$, where $\tilde{\Omega}$ is the characteristic energy of the Eliashberg function, the expression (3) has a form

$$W = \gamma^{\text{imp}} + 2\pi\lambda\beta T,$$

where the transport coupling constant λ is defined by the standard relation

$$\lambda = 2 \int_0^\infty d\Omega \frac{\alpha^2(\Omega)F(\Omega)}{\Omega}. \quad (6)$$

In this regime

$$\rho_{DC}(T) = \left[\frac{\epsilon_0 \omega_{pl1}^2}{\gamma_1^{\text{imp}} + 2\pi\lambda_1\beta T} + \frac{\epsilon_0 \omega_{pl2}^2}{\gamma_2^{\text{imp}} + 2\pi\lambda_2\beta T} \right]^{-1}, \quad (7)$$

where the effective coupling constants are defined as $\lambda_1 = \lambda_{11} + \lambda_{12}$ and $\lambda_2 = \lambda_{21} + \lambda_{22}$ and

$$\lambda_{ij} = 2 \int_0^\infty d\Omega \frac{\alpha_{ij}^2(\Omega)F_{ij}(\Omega)}{\Omega}. \quad (8)$$

In the two band model the saturation of the resistivity has the following explanation. First, there exists large disparity between the coupling constants in $\text{Ba}_{1-x}\text{K}_x\text{Fe}_2\text{As}_2$: $\lambda_1 \gg \lambda_2$. This fact follows from the quantitative analysis of thermodynamic data presented in Ref. [19]. Second, Hall effect data presented in Ref. [13] suggest that $\gamma_2^{\text{imp}} \gg \gamma_1^{\text{imp}}$. Though calculation of these scattering rates is beyond the framework of the present paper, we consider this relation between the scattering parameters as a reasonable assumption in the two-band model for $\text{Ba}_{1-x}\text{K}_x\text{Fe}_2\text{As}_2$. As a result, combining the conditions $\lambda_1 \gg \lambda_2$ and $\gamma_2^{\text{imp}} \gg \gamma_1^{\text{imp}}$ we arrive the expression

$$\rho_{DC}(T) = \left[\frac{\epsilon_0 \omega_{pl1}^2}{\gamma_1^{\text{imp}} + 2\pi\lambda_1\beta T} + \frac{\epsilon_0 \omega_{pl2}^2}{\gamma_2^{\text{imp}}} \right]^{-1}, \quad (9)$$

which is valid in a broad temperature range $T < \gamma_2^{\text{imp}}/2\pi\lambda_2\beta$. As follows from the above expression, the resistivity saturates at $T > \gamma_2^{\text{imp}}/2\pi\lambda_1\beta$ up to the value

$$\rho_{DC}(T) = \frac{\gamma_2^{\text{imp}}}{\epsilon_0 \omega_{pl2}^2}.$$

This saturation manifests itself as the crossover from the standard Bloch–Grüneisen temperature dependence of the resistivity to the behavior characterized by the downward curvature of the $\rho(T)$ curve, with the crossover temperature $T^* \simeq \gamma_2^{\text{imp}}/2\pi\lambda_1\beta$.

Thus, we have shown that at high temperatures the conductivity of the second band shunts the conductivity of the first one, leading to the saturation of the total resistance (see Eq. (1)). Below we apply this model to describe the experimental data for the resistivity of $\text{Ba}_{1-x}\text{K}_x\text{Fe}_2\text{As}_2$ compound.

Comparison with experiment and discussion.

The transport properties of hole-doped $Ba_{1-x}K_xFe_2As_2$ single crystals in normal and superconducting state were studied by two different techniques: by measuring the microwave surface impedance and by measuring dc -resistivity. The measurements were carried out on single crystals of $Ba_{1-x}K_xFe_2As_2$ (BKFA) with $x = 0.32$ and superconducting $T_c = 38.5$ K. Specific heat measurements on the same samples confirm their high quality and the absence of secondary electronic phases [19].

The temperature dependence of the surface impedance of the $Ba_{1-x}K_xFe_2As_2$ single crystals were measured by the “hot finger” technique at frequency 9.42 GHz. The experimental setup involved a cylindrical cavity niobium resonator operating at the mode H_{011} . The walls of the resonator are cooled down with liquid helium and are in the superconducting state. The crystal was placed at the end of the sapphire rod in a uniform high-frequency magnetic field, so that microwave currents flow along the superconducting layers of the crystal. The temperature of the rod and the sample can be varied in the range from 5 to 300 K.

In the temperature range $40 < T < 80$ K one can see normal skin effect: the real (surface resistance $R(T)$) and imaginary (reactance $X(T)$) parts of the surface impedance are equal, $R(T) = X(T)$ (see Fig. 1). At $T >$

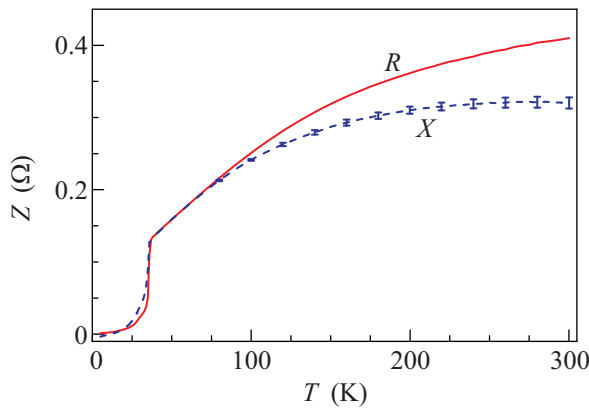


Fig. 1. Surface resistance (R) and reactance (X) in the conducting layers of a $Ba_{1-x}K_xFe_2As_2$ single crystal at frequency 9.42 GHz. Sample size is $1.65 \times 0.8 \times 0.06$ mm³

80 K the reactance $X(T)$ becomes less than $R(T)$, which is most likely due to thermal expansion of the crystal [22]. Fig. 2 shows temperature dependence of the resistivity found from the expression $\rho(T) = 2R^2(T)/\omega\mu_0$ valid for a homogeneous conductor.

The dc -resistivity measurements were carried out in the temperature range $4.2 < T < 280$ K. The samples were thin plates with $1.8 \times 0.8 \times 0.02$ mm³ characteristic size. The largest surface of the plate was oriented

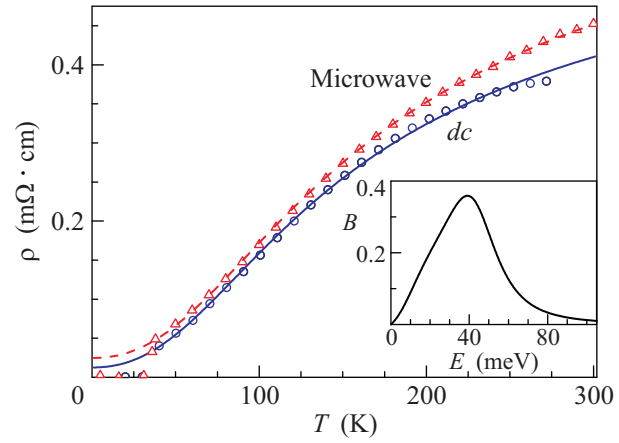


Fig. 2. Theoretical fits to resistivity of $Ba_{1-x}K_xFe_2As_2$ single crystals determined from dc and microwave measurements. The fitting parameters are given in the text

along the conducting layers. The sample resistance was measured using a four-probe technique by a lock-in detector at 20 Hz alternating current. The contacts were prepared on the sample surface with conducting silver paste. The in-plane resistivity component $\rho(T)$ is characterized by anomalous T -dependence: $\rho(T)$ curve is convex with the tendency to saturate at high temperature, i.e. similar to the $R(T)$ dependence measured at microwave frequency.

The results of comparison between theory and experiment are shown in Fig. 2. Important parameters in the present model are impurity scattering rates in each band. As is seen from the figure, the results of measurements are consistent with the scenario when the first (strongly coupled) band has much smaller scattering rate than the second one. Indeed, in accordance with theoretical picture described above, resistivity saturation occurs when two conditions, $\lambda_1 \gg \lambda_2$ and $\gamma_2^{\text{imp}} \gg \gamma_1^{\text{imp}}$, are fulfilled.

In the framework of spin-fluctuation pairing mechanism [8–10], nesting between electron and hole pockets is important for superconductivity. Such nesting conditions are realized for inner hole pocket and electronic pockets, but are not fulfilled for the outer hole pocket. Therefore, as was pointed out above, the second band is characterized by much weaker pairing interaction than the first one. Our fitting parameters are in qualitative agreement with this scenario, namely $\lambda_1 = 1.8$, $\lambda_2 \simeq 0$. The scattering rates obtained from the fitting are: $\gamma_1^{\text{imp}} = 3$ meV, $\gamma_2^{\text{imp}} = 67$ meV (for the dc resistivity fit) and $\gamma_1^{\text{imp}} = 6$ meV, $\gamma_2^{\text{imp}} = 78$ meV (for the microwave resistivity fit). The differences between the dc and microwave resistivity fits can be attributed to the fact that microwave impedance measure-

ment is surface sensitive technique. Plasma frequencies were chosen as $\omega_{p1} = 1.33$ eV and $\omega_{p2} = 0.87$ eV and are consistent with optical measurements [23] were total plasma frequency of 1.6 eV was determined. The transport Eliashberg function was chosen in the form $\alpha_i^2(\Omega)F(\Omega) = \lambda_i B(\Omega)$, where the function $B(\Omega)$ is shown in the inset in Fig. 2. With the above parameters, the crossover temperature $T^* \simeq \gamma_2^{\text{imp}}/2\pi\lambda_1\beta \sim 100$ K. The estimated value of the Fermi energy E_F is equal to 0.6 eV at $T = 300$ K. Therefore, up to the highest temperatures the Ioffe–Regel limit in energy units $E_F \sim (\gamma_i^{\text{imp}} + 2\pi\lambda_i\beta T)$ is not reached for both bands and localization effects (neglected in our model) are not important. Note also that despite a number of free parameters, the present model provides rather unique fit, since the crossover only occurs in narrow parameter range, corresponding to strong, about an order of magnitude, disparity of the scattering rates and the coupling strengths in both bands.

The multiband scenario, applied above to explain the resistivity anomaly at high temperatures, is also consistent with our results of Hall effect measurements on the same set of samples shown in Fig. 3. One can see that

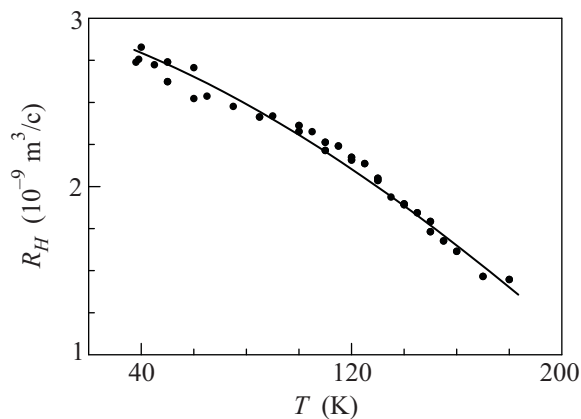


Fig. 3. The temperature dependence of the Hall constant in a $\text{Ba}_{1-x}\text{K}_x\text{Fe}_2\text{As}_2$ single crystal. Solid line is a guide to an eye

Hall constant R_H decreases with increasing temperature. The temperature dependent R_H value was also observed recently [12, 13] in Co-doped and K-doped compounds. Though detailed quantitative description of the behavior of the Hall constant is beyond the framework of the present work, qualitative discussion was given in Ref. [13]. As is argued in [13], the temperature dependence of R_H is naturally explained by the mobility changes, because in multi-band conductors R_H value is the function of both concentration and mobility.

The difference in resistivity behavior between K- and Co-doped samples has natural explanation in the frame-

work of our model. The transition temperature in Co-doped pnictides is reduced, which can be attributed to weaker coupling constant λ_1 in the first band. Within our scenario, that means that the crossover temperature $T^* \simeq \gamma_2^{\text{imp}}/2\pi\lambda_1\beta$ is higher than in the K-doped case considered above. As a result, the regime of the resistivity saturation in Co-doped pnictides should shift to higher temperatures.

In conclusion, we have presented two-band Eliashberg model for the normal-state resistivity in iron-pnictides, which naturally explains the observed tendency to resistivity saturation and temperature-dependent Hall coefficient in K- and Ru-doped BaFe_2As_2 , as well as in LiFeAs and SrPt_2As_2 compounds. The results are in a good agreement with *dc* and microwave resistivity measurements in $\text{Ba}_{0.68}\text{K}_{0.32}\text{Fe}_2\text{As}_2$ single crystals with $T_c = 38.5$ K. This analysis reveals strong disparity of relaxation rates and strongly different coupling constants in different bands in these materials.

We acknowledge useful discussions with V.F. Gantmakher, R.K. Kremer, I.I. Mazin, and A.N. Yaresko. This work was supported by the Grant # 2009-1.5-508-008-043 within the Federal program funded by Russian Ministry of Education and Science and by RFBR grants # 09-02-01224 and 11-02-12071.

1. H. J. Mooij, *Phys. Stat. Sol. a* **17**, 521 (1973).
2. Z. Fisk and G. W. Webb, *Phys. Rev. Lett.* **36**, 1084 (1976).
3. M. Gurrich, *Phys. Rev. B* **24**, 7404 (1981).
4. V. F. Gantmakher, *Electrons and Disorder in Solids*, Oxford University Press, 2005.
5. M. Milewits, S. J. Williamson, and H. Taub, *Phys. Rev. B* **13**, 5199 (1976).
6. Yu. A. Nefyodov, A. M. Shuvaev, and M. R. Trunin, *Europhys. Lett.* **72**, 638 (2005).
7. Y. Kamihara, T. Watanabe, M. Hirano, and H. Hosono, *J. Am. Chem. Soc.* **130**, 3296 (2008).
8. I. I. Mazin, D. J. Singh, M. D. Johannes, and M. H. Du, *Phys. Rev. Lett.* **101**, 057003 (2008).
9. K. Kuroki, S. Onari, R. Arita et al., *Phys. Rev. Lett.* **101**, 087004 (2008).
10. I. I. Mazin, *Nature* **464**, 183 (2010).
11. D. C. Johnston, arXiv:1005.4392 (unpublished).
12. F. Rullier-Albenque, D. Colson, A. Forget, and H. Al-loul, *Phys. Rev. Lett.* **103**, 057001 (2009).
13. L. Fang, H. Luo, P. Cheng et al., *Phys. Rev. B* **80**, 140508(R) (2009).
14. H. Q. Luo, P. Cheng, Z. S. Wang et al., *Physica C* **469**, 477 (2009).

15. V. N. Zverev, A. V. Korobenko, G. L. Sun et al., JETP Letters **90**, 130 (2009).
16. O. Heyer, T. Lorenz, V. B. Zabolotnyy et al., arXiv:1010.2876 (unpublished).
17. F. Rullier-Albenque, D. Colson, A. Forget et al., Phys. Rev. B **81**, 224503 (2010).
18. K. Kudo, Y. Nishikubo, and M. Nohara, arXiv:1010.3950 (unpublished).
19. P. Popovich, A. V. Boris, O. V. Dolgov et al., Phys. Rev. Lett. **105**, 027003 (2010).
20. G. Grimvall, *The electron-phonon interaction in metals*, North-Holland, 1981.
21. P. B. Allen, Phys. Rev. B **3**, 305 (1971).
22. M. R. Trunin, Sov. Phys. Uspekhi **168**, 931 (2005).
23. A. Charnukha, O. V. Dolgov, A. A. Golubov et al., arXiv: 1103.0938.